





Article

Synthesis, Characterization, and Antibacterial Efficacy of Borosilicate Compound against *Escherichia coli*

Bertha Silvana Vera Barrios ^{1,*}, Elisban Juani Sacari Sacari ², Ramalinga Viswanathan Mangalaraja ^{3,4,*}, Arunachalam Arulraj ⁵, Isabel del Carmen Espinoza Reynoso ⁶, Teresa Cano de Terrones ⁷, Josué Amílcar Aguilar Martínez ⁸, Fabrizio del Carpio Delgado ⁹ and Luis Antonio Lazo Alarcón ¹⁰

- ¹ Facultad Ing. de Minas, Universidad Nacional de Moquegua, Moquegua 18001, Peru
- ² Nanotechnology Laboratory, Facultad de Ingeniería, Universidad Nacional Jorge Basadre Grohmann, Avenida Miraflores S/N, Ciudad Universitaria, Tacna 23003, Peru; esacaris@unjb.edu.pe
- ³ Faculty of Engineering and Sciences, Universidad Adolfo Ibáñez, Diagonal las Torres 2640, Peñalolén, Santiago 7941169, Chile
- ⁴ Department of Mechanical Engineering, Faculty of Engineering, Karpagam Academy of Higher Education, Coimbatore 641 021, Tamil Nadu, India
- ⁵ Departamento de Electricidad, Facultad de Ingeniería, Universidad Tecnológica Metropolitana (UTEM), Santiago 7800002, Chile; arul@utem.cl
- ⁶ Department of Biology, ONG Waykay, Ilo 18601, Peru; isabelita@gmail.com
- ⁷ Department of Chemistry, Universidad Nacional de San Agustín, Arequipa 68513, Peru; dcanof@unsa.edu.pe
- ⁸ Facultad de Ingeniería Mecánica Eléctrica-FIME, Universidad Autónoma de Nuevo León, Monterrey 66455, Mexico; josue.aguilar74@gmail.com
- ⁹ Laboratory of Materials, Universidad Nacional de Moquegua, Moquegua 18001, Peru; fabiunam@gmail.com
- ¹⁰ Laboratory of Materials, Universidad Nacional de San Agustín, Arequipa 68513, Peru; luisitolazo@gmail.com
- * Correspondence: anavlisarev@gmail.com (B.S.V.B.); mangal@uai.cl (R.V.M.)



Citation: Vera Barrios, B.S.; Sacari Sacari, E.J.; Mangalaraja, R.V.; Arulraj, A.; Espinoza Reynoso, I.d.C.; Cano de Terrones, T.; Aguilar Martínez, J.A.; del Carpio Delgado, F.; Lazo Alarcón, L.A. Synthesis, Characterization, and Antibacterial Efficacy of Borosilicate Compound against *Escherichia coli*. *Processes* **2023**, *11*, 3414. <https://doi.org/10.3390/pr11123414>

Academic Editor: Bing-Huei Chen

Received: 3 September 2023

Revised: 30 October 2023

Accepted: 14 November 2023

Published: 13 December 2023



Copyright: © 2023 by the authors. Licensee MDPI, Basel, Switzerland. This article is an open access article distributed under the terms and conditions of the Creative Commons Attribution (CC BY) license (<https://creativecommons.org/licenses/by/4.0/>).

Abstract: In this study, a glassy borosilicate compound was synthesized using recycled glass and natural clays. Even though glass recycling is the generally accepted standard practice for managing glass waste, fine fractions of container soda-lime glass or cullet of other compositions are still disposed of in landfills. Thus, advanced upcycled products that offer greater economic motivation for implementation in industry may be the key to success, but these are frequently linked to alternative methods of product synthesis. Here, a simple and facile route of borosilicate compound production has been synthesized and characterized. The physicochemical characterization of the compounds was carried out to determine their properties and the antibacterial efficacy of the synthesized compound against *Escherichia coli* (*E. coli*) was investigated. The structural and spectroscopic characteristics were identified as a compound that conformed to quartz, cristobalite, and silicon hexaboride (SiB₆). For the antibacterial activity, two test types were typically performed; in the first one, the dilutions of the grind were combined with chloramphenicol at a concentration of 20 µg/mL to perform a synergistic action against the bacteria and in the second one, only the amorphous borosilicate compound was tested against *E. coli* ATCC 25922 strains. The treatments applied considered the dilutions from 8 to 40 µg/mL. The minimum inhibitory concentration (MIC) sensitivity tests began with incubation at 37 °C in the tubes and subsequent seeding in Petri dishes for colony-forming unit (CFU) counting. The results obtained indicated that the samples possessed a productive antibacterial effect, which support their use in various biomedical applications.

Keywords: borosilicate; amorphous; antibacterial; *E. coli*; chloramphenicol

1. Introduction

Waste materials, both hazardous and non-hazardous, are most often associated with industrial processes, production, and human activities. Therefore, it is crucial to recycle and reprocess such wastes to maximize economic gains and safeguard the environment. Recycling is the process of choosing, sorting, and using waste again as a primary resource

to create a product that is identical to or extremely comparable to the original material. In this respect, the rise in product consumption and rigorous emphasis on high-quality manufacture are the main causes for the elevation in the production of enormous volumes of glass waste per year [1,2]. Each year, thousands of tons of glass are landfilled, even though 76% of glass waste is recycled in the EU1 and 33% in North America. Fine fractions (fibers and their composites) can be found in glass soda-lime cans, even those that are recycled the most [2,3]. Also, if a product is poor, such glasses are frequently landfilled right after they are manufactured. For environmental preservation, glass wastes should also receive careful consideration, as they take millions of years to decompose in nature. Therefore, the recycling of glass is a significant subject that needs to be researched, as it has the potential to have both positive economic and environmental effects. There are several strategies for recycling glass waste into valuable products. Recycled glass, particularly borosilicate, exhibits the characteristics of low thermal expansion coefficient and dielectric constant, high electrical conductivity, and hydrolytic resistance [4–6]. Such borosilicate (BS) compounds are applied in medical, structural, and antibacterial usages, bioactive glasses, and also for developing tissue engineering applications [7].

There are several borate compounds that have been found to be potential candidates for various applications in the medical field [8]; for instance, icosahedral boron cluster compounds have good stability and bioavailability, and are the most commonly used structures of this class in drug development. Boron cluster compounds have the potential to become viable and suitable candidates for antimicrobial therapy. The combination of ethylenediaminetetraacetic acid (EDTA) with boric acid to treat and/or prevent vaginal infections is due to its role as a disruptor of the vaginal biofilm. Boric acid can also be used in the methodology for treating vaginal infections, which is selected from bacterial infections and trichomoniasis [9], constituting the possibilities for several medical applications. The antibacterial effects of boric acid, unlike many antibiotics, appear to be independent of cell growth, as dividing and stationary phase cells are affected. Under two photoperiod conditions (dark and light), a concentration of 9.3 mg L^{-1} of boric acid was evaluated under in vitro culture conditions [10]. Likewise, the incorporation of copper (Cu) and silver (Ag) with bioactive glass led to an innovative methodology in tissue engineering. For instance, improved electroactive, mesoporous, and Ag-doped bio-ceramics for medical usages have been developed, and their structural, electrical, in vitro bioactivity, cell culture, and antibacterial properties against pathogenic bacteria were determined and reported [11]. On the other hand, copper–borosilicate and borosilicate glasses inhibit *E. coli* growth, and three kinds of bioactive glass particles (silicate, borosilicate, and copper–borosilicate) have been added as a second phase to hybrid organic–inorganic silica-based sol-gel coatings to improve the surface properties of stainless steel as an implant material [12]. Developed borosilicate compounds with the structural and bioactivity properties of a phosphate-free novel composition of calcium borosilicate mesoporous glass–ceramic have been reported [13]. A few hundred parts per million of boron/boric acid in bentonitic clays can affect the reduction in bacterial colonies. Sol-gel-synthesized boron nitride (BN) thin films for antibacterial and magnetic applications demonstrated that the derivatives have remarkable antibacterial activity against bacterial strains of *E. coli* [14]. Similarly, the application of boric acid to a bacterium called “*Pseudomonas putida* strain KT2440” showed effects on its growth and activity, but at concentrations of 40 mM [15].

Chloramphenicol, despite being an antibiotic of medium intensity, can be assimilated to reinforce defensive activity, and that is the reason why it was included in this research. The action mechanism of chloramphenicol against *E. coli* is generally reported to be bacteriostatic, but it can be bactericidal at high concentrations or against highly susceptible organisms, such as *Haemophilus influenza* (*H. influenza*) and *Streptococcus pneumoniae* (*S. pneumoniae*). Chloramphenicol, a broad-spectrum antibiotic, can be used against a wide range of Gram-positive and Gram-negative bacteria. In vitro concentrations of 0.1 to 20 $\mu\text{g/mL}$ of chloramphenicol are generally effective against susceptible strains. Owing to its hematological toxicity related to serum concentrations, it is not recommended to reach

peak concentrations higher than 25 µg/mL [16,17]. Chloramphenicol is an antibiotic that is not prescribed as a first choice, but it can be an important alternative in specific cases where others are not suitable for the treatment of infections or in patients allergic to beta-lactams (β-lactams) [18], reports indicate that it does fight *E. coli*, but has a resistance of 35%, i.e., chloramphenicol is only 70% effective against *E. coli* [19]. Also, the literature review established a MIC for chloramphenicol of 8 mg/mL as very sensitive, while it indicated 20 mg/mL, both against *E. coli*, in dilution media; it could be proven that neither of them is applicable, since it has been demonstrated by experimentation that these proportions are not effective to combat *E. coli* when they act jointly with BSC, which is the primary objective of the study carried out in this research. Finally, it could be reported from the results that chloramphenicol is not effective against "*Aeromonas*" bacteria that affect the digestive system, as well as *E. coli*, when the concentrations are between 8 and 32 mg/mL [17].

Thus, in this work, an improved and ecological substance was designed to be used as an "antibacterial borosilicate compound", and the main aim was focused on studying this substance, which was obtained mainly from recycled waste boron, ground glass particles, and residual clays. As aforementioned, boron is one of the chemical elements that is the most important to preparing the compound, and its importance is rising owing to its multifunctional applications. Such an element can appear naturally in soils and rocks, but it is also found on water surfaces polluted with boric acid and inorganic borates. Therefore, herein, the antibacterial efficacy of a "borosilicate compound" synthesized from recycled glasses and natural clays, made of boron, aluminosilicates, and silicon dioxide, was determined through studying the values of the MIC in µg/mL against *E. coli* ATCC 25922 strains. For this purpose, two substances were used to test the combined action of the powdered borosilicate compound with another antibiotic, "chloramphenicol", in order to compare its antibacterial efficacy.

2. Material and Methods

2.1. Synthesis of Borosilicate (BSAS and BSC) Compounds

Given that this material is intended to be used in pavements, some of its components are of natural origin and, in turn, recycled materials, such as clay and glass from the glass industry in the city of Arequipa, Peru. The borosilicate compound (BSC) was synthesized using 10 g of natural clay obtained from "Canteras Lajas Arequipa, Peru", 20 g of kaolin (Química Industrial, Lima, Peru), 30 g of sodium tetraborate decahydrate (Procampo, Lima, Peru), 20 g of boric acid (Inkabor, Lima, Peru), 4 g of quartz (Química Industrial, Lima, Peru), 6 g of recycled glass, 0.6 g of yellow pigment (Baycolor, Lima, Peru), and 9.6 g of white marble pigment (Baycolor, Lima, Peru). The materials were mixed and ground without further purification for 14 h by adding 500 mL of distilled water, ground, and then dried at room temperature; the collected material was ground and passed through a 200 mesh and labeled as "prepared borosilicate" (BSAS). Then, the obtained sample was calcined at 980 °C for 14 h and ground and passed through the 200 mesh. Finally, the obtained product (sample) was labeled as calcined borosilicate (BSC).

2.2. Materials Characterization

The thermal properties of the BSAS samples were studied by simultaneous differential heat flow by using an SDT 650 (TA instruments, New Castle, DE, USA) differential scanning calorimetry and thermogravimetric analyzer (DSC/TGA) from room temperature to 1000 °C at a 20 °C/min heating rate under a nitrogen (N₂) atmosphere. The structural characterization of the samples (BSAS and BSC) was performed using an X-ray diffractometer, model D8 Focus (Bruker, Coventry, UK), with Cu-K_α radiation (1.5406 Å) operated at 30 kV and 30 mA. The diffraction patterns were recorded from 5° to 70° with steps of 0.011° and 8.67 s per step. The functional groups of the samples were analyzed by using Fourier-transform infrared (FTIR) analysis and the spectra were recorded utilizing a Bruker Invenio R spectrometer (Bruker, Ettlingen, Germany). The morphological and elemental

analyses were performed by using scanning electron microscopy (SEM), model Scios2 (Thermo Scientific Co., Eindhoven, The Netherlands).

2.3. Antibacterial Experimental Procedure

The procedure consisted of using an inoculum of *E. coli* ATCC 25922 to perform the MIC test in the tubes, incubating at 37 °C, and successive sowing in Petri dishes for CFU counting. Two stages were developed; in the first one, different quantities of BSC were dispersed in concentrations that increased with each other in 20 µg/mL, of which one part was BSC and the other was chloramphenicol, against a Gram-negative *E. coli* bacterium. The concentration was as follows: for each 10 mL of peptone solution, different weight proportions of 8, 12, 16, 20, and 24 µg/mL of the BSC were added with the antibiotic substance chloramphenicol, making a total of 7 specimens with these combinations and 1 blank specimen. All the procedures carried out in the first stage were called “Mix 01” and all those carried out in the second stage were called “Mix 02” (Figure 1).

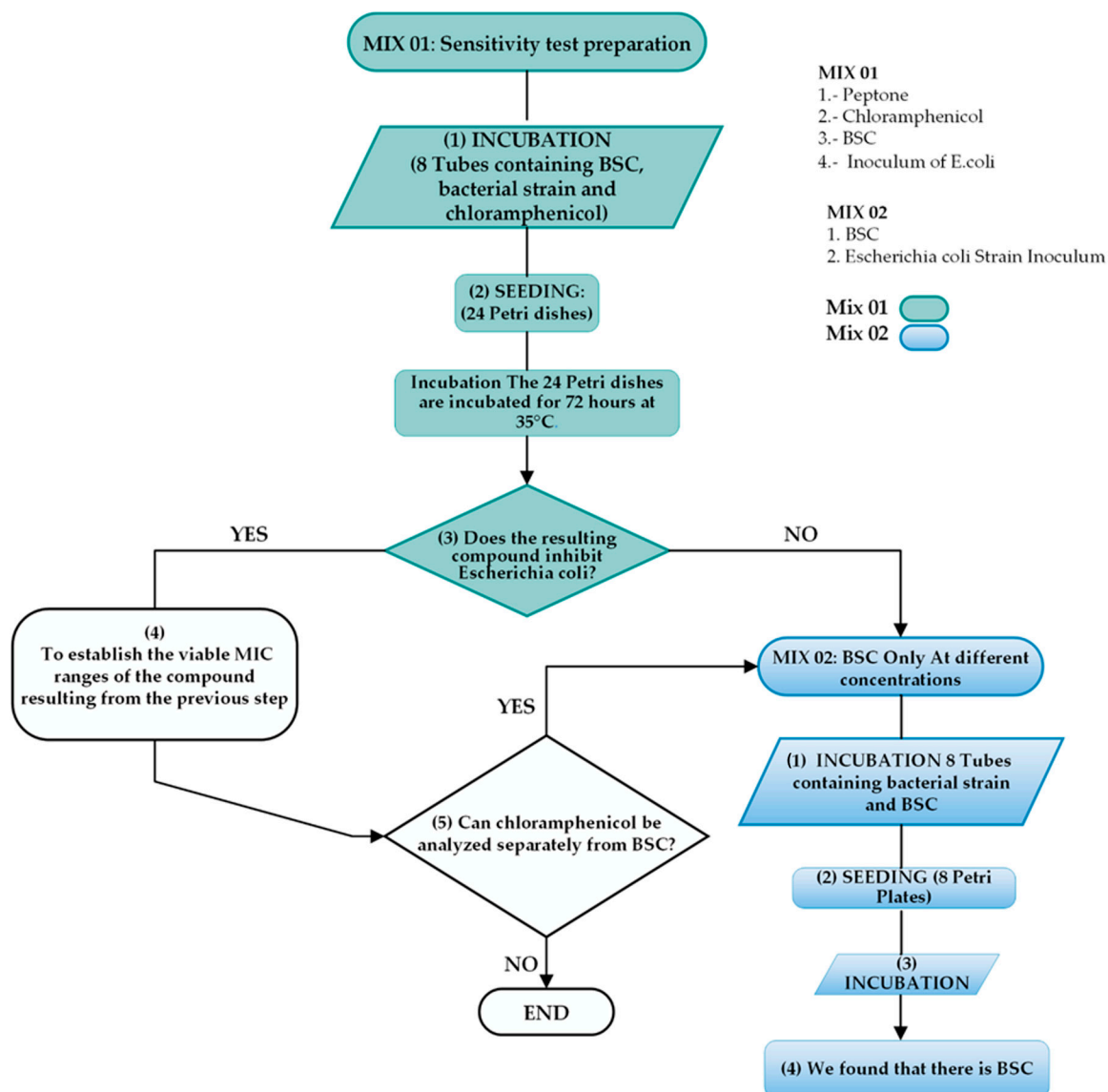


Figure 1. Flowchart describing the antibacterial test.

2.3.1. Stage 1

In the first stage, eight combinations were prepared, in which the first and the last were control samples. Sample 1 contained only chloramphenicol and sample 8 was the blank sample. In each of the remaining 6 combinations, BSC was added in increasing proportions, and the other substance, chloramphenicol, had a constant volume of 20 µg/mL. Sample 7 was the standard sample because it was the one that contained only the BSC in powder form, where 100% of it was the compound and chloramphenicol accounted for 0%. All samples from 1 to 6 contained both chloramphenicol and BSC simultaneously. The amount of peptone by volume was constant for all 7 combinations, as was the concentration of peptone. The products were weighed into sterile empty tubes; chloramphenicol was weighed first and added to tubes 1 to 6 (in triplicate) at 20 µg/mL. Next, the BSC was added in the indicated amounts and then, in a sterile seeding chamber, 10 mL of 0.1% peptone was added to each tube, including the series already mentioned, with tube 7 as the standard (in this case, only 3 repetitions were performed) and 8 as the blank. To the eight series of three tubes (24 tubes), 1 mL of strain inoculum was added. Three tubes were added as a negative control in which no inoculum was added and that only contained 0.1% of sterile peptone.

2.3.2. Stage 2

The next step was “incubation”; once the preparation was completed, the tubes were placed in a rack in a calibrated incubator at 37 °C for 3 days (72 h). The tubes were only taken out of incubation every 24 h to capture photographs and detect the variations in their characteristics, if any. Afterward, the “seeding” stage continued, the incubation tubes were removed and taken back to the sterile seeding chamber; the whole process was carried out in the presence of a lit burner and with sterile material (Figure 1).

With respect to the tubes, each tube was inoculated onto Petri film plates following the procedure; with a sterile pipette, 1 mL was extracted from each tube after the homogenization of its contents, placed in the Petri film *E. coli* plate by lifting the upper film and applying it to the culture medium of the Petri film before returning the upper film to the culture medium. The Petri film *E. coli* plates were allowed to stabilize for five minutes. In addition, decimal dilutions were prepared, and each was inoculated onto a fresh Petri film plate. The *E. coli* Petri film plates were labeled with the corresponding tube code and dilution. Each dilution was prepared with 9 mL of sterile 0.1% peptone and 1 mL of the previous dilution. Eleven dilutions of each tube were used (except for the negative control, where only one direct sample was used). Then, returning to the “incubation” stage, the Petri film plates with *E. coli* were incubated at 35 °C for 48 h in a calibrated incubator.

2.3.3. Stage 3

Next came the “Reading” stage; all plates were checked and those with between 15 and 150 colonies were counted. The *E. coli* colonies were blue dots and were associated with a gas bubble. The counts obtained were reported and expressed in CFU/mL. In the second part, 9 concentrations and/or samples representing different concentrations of BSC above and below 20 µg/mL were used. These samples were designed by maintaining an arithmetic progression with the following concentrations: 8, 12, 16, 20, 24, 28, 32, 36, and 40 µg/mL, producing a total of 9 samples. The design criteria of the conditions for the methodological procedure were also kept constant, such as the uniform inoculum size, temperature, and the culture or sowing times of the previous stage; however, the number of samples was modified since, in this stage, there were 9, so the positive and negative control samples were eliminated as these results were already known according to the previous stage, and 3 groups were analyzed again; therefore, only 27 results are available, in each of which a volume of 790,000 microorganisms of *E. coli* was inoculated and left for 72 h. The antibacterial activities against *E. coli* microorganisms (for the 72 h inoculated samples) were examined to observe the replications of the number of microorganisms (kindly refer to Section 3.5) to perform a more thorough evaluation of the number of

surviving microorganisms on each day of evaluation. All the conditions used in the previous stage in terms of temperature, strain, peptone, etc., were used again.

3. Results

3.1. Thermal Analysis

The thermal characteristics of the BSAS sample were determined using TGA/DSC analysis and are presented in Figure 2. The sample presented four stages from room temperature to 1000 °C; the first reaction occurred from room temperature to 127 °C, when there is a decrease in weight of ~10% and an exothermic reaction that corresponded to the evaporation of humidity and water contained in the sample. The second stage appeared from 127 to 216 °C, with a weight loss of ~21% and an endothermic reaction with a peak shoulder that corresponded to the dehydration of boric acid and its boiling [20]. The third stage occurred from 216 to 634 °C, where an exothermic peak appeared that corresponded to the evaporation of the boric acid and the volatilization of the organic compounds present in the pigments, with a total weight loss of ~25%. From 634 to 900 °C, the total weight loss was ~26%, and an endothermic flat reaction happened that could be related to the boiling of the sodium tetraborate decahydrate. From 900 to 1000 °C, an exothermal peak occurred that could be attributed to the remaining boron on the silicon dioxide (SiO_2) surface diffusing through the SiO_2 , forming the most favorable phase of SiB_4 , but with the excess boron that transformed to SiB_6 [21], with a total weight loss of ~27% at 1000 °C.

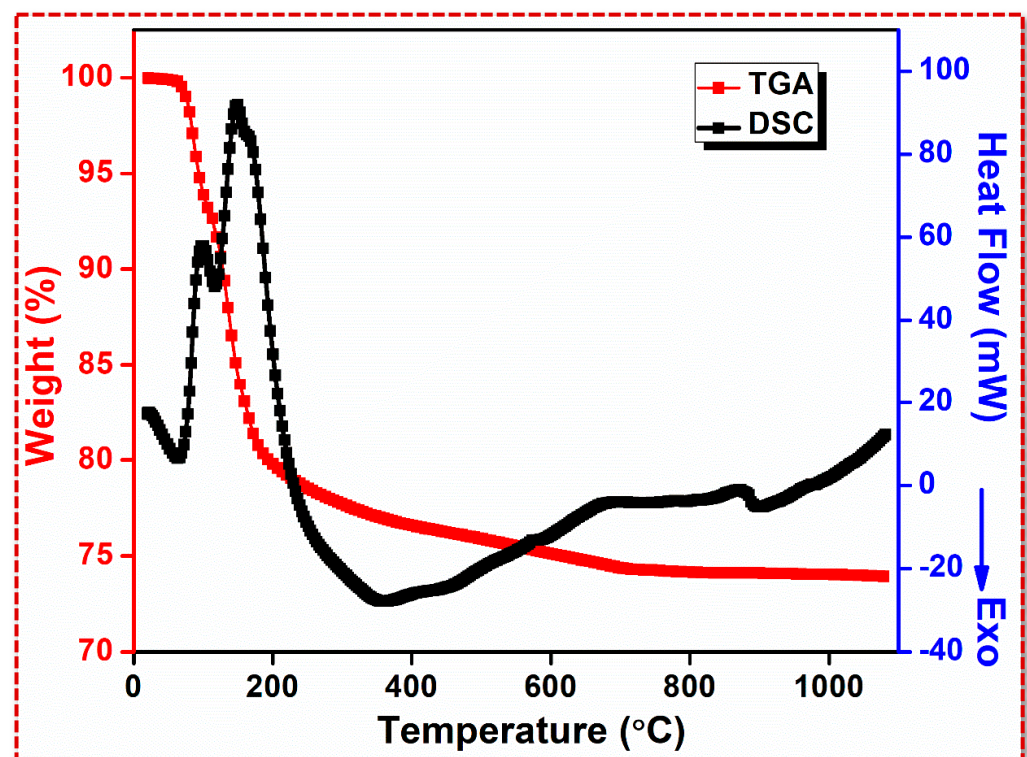


Figure 2. TGA and DSC curves of BSAS sample.

3.2. Phase and Structural Analysis

Figure 3 shows the XRD patterns obtained for the BSAS and BSC samples. The BSAS sample was composed principally of three phases; the principal phase has characteristics peaks located at 2θ values of 15.2° and 28° that correspond to boric acid in the Sassolite phase (JCPDS No.: 01-0767) and the second phase had peaks located at 2θ values of 12.4° , 18.3° , 24.8° , 31.4° , and 47.9° that corresponded to sodium tetraborate decahydrate (JCPDS No.: 24-1055), commonly called Borax.

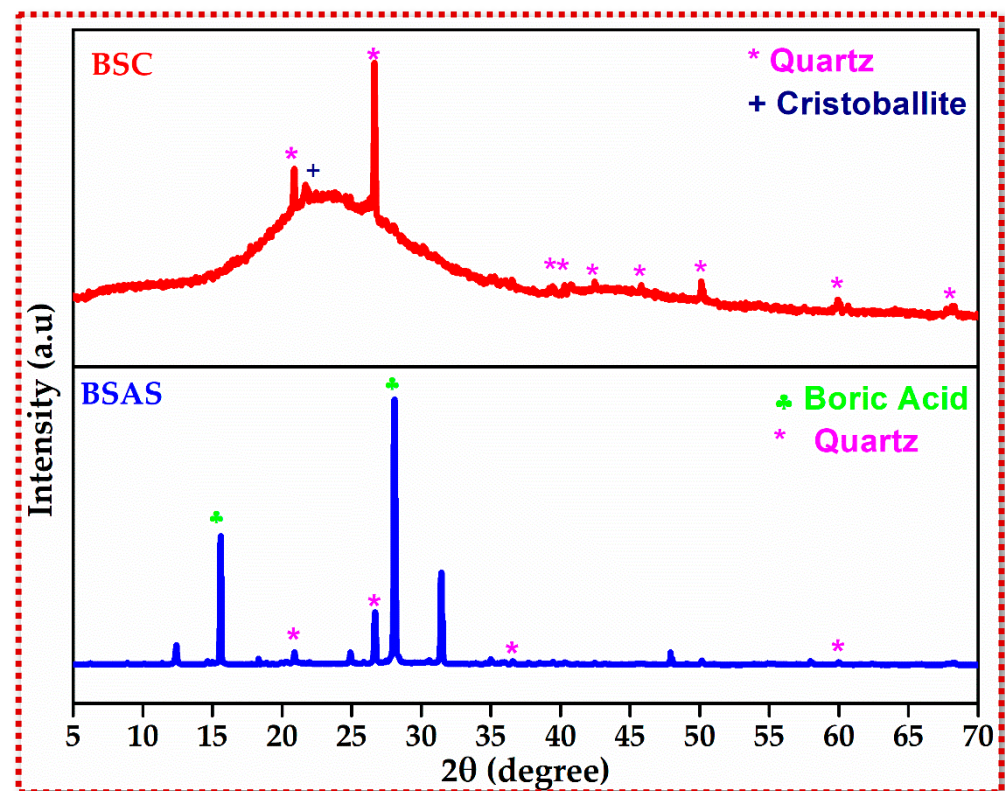


Figure 3. XRD patterns of BSAS and BSC samples.

The third phase had peaks located at 2θ values of 20.8° , 26.7° , 36.6° , and 60.1° , which corresponded to the SiO_2 in the quartz phase (JCPDS No.: 87-2096). The results also indicated that the calcined samples had two crystalline phases and one amorphous phase; the diffraction peaks located at 2θ values of 20.8° , 26.6° , 39.4° , 40.3° , 42.4° , 45.7° , 50.16° , 59.9° , and 68.1° were in good agreement with the quartz phase of SiO_2 (JCPDS No.: 87-2096). A short peak located at a 2θ value of 21.7° corresponded to the cristobalite phase of SiO_2 (JCPDS No.: 27-0605); additionally, around $15\text{--}40^\circ$, a prominent hump typically appeared that corresponded to the amorphous material present in the sample, which could be attributed to SiB_6 that may have been formed by mixing boric acid and sodium tetraborate decahydrate with silicon oxide, forming networks in which boron replaced oxygen in the SiO_2 network [22]. A Rietveld quantitative phase analysis of the BSC sample was performed using Highscore Plus software version 4.8 (PANalytical, Almelo, The Netherlands) [23]. A shifted Chebyshev method was used to adjust the background intensity. The crystalline and amorphous phase contents obtained from the Rietveld refinement technique were 62.1% quartz, 6.6% cristobalite, and 31.3% amorphous, with $R_{\text{exp}} = 4.3039$, $R_p = 3.8892$, $R_{\text{wp}} = 6.4488$, and GOF 1.49.

3.3. Functional Group Analysis Using FTIR

Figure 4 shows the FTIR absorption spectra recorded for the BSAS and BSC samples. According to the results obtained for the BSAS sample, the peaks at 3797 , 3619 , 1039 , 908 , and 540 cm^{-1} could be attributed to the SiO_2 in the quartz phase, the bulge at $3300\text{--}3600\text{ cm}^{-1}$ and the peaks at 1407 and 1180 cm^{-1} were related to the sodium tetraborate decahydrate, and the peaks located at 3240 , 2365 , 2282 , and 3619 cm^{-1} could be attributed to boric acid. The results for the BSC sample indicate that the material had the principal contributions of peaks located at 1407 , 1071 , 798 , and 454 cm^{-1} corresponding to SiB_6 and a contribution of SiO_2 , with peaks located at 540 and 3438 cm^{-1} ; the shoulder peaks at 1440 , 775 , and 450 cm^{-1} could be attributed to the small contribution of remnant sodium tetraborate [24,25]. The analysis of the data shows that the final product was

composed principally of amorphous SiB_6 and SiO_2 in the quartz phase, which is consistent with the results obtained in the X-ray diffraction (XRD) analysis.

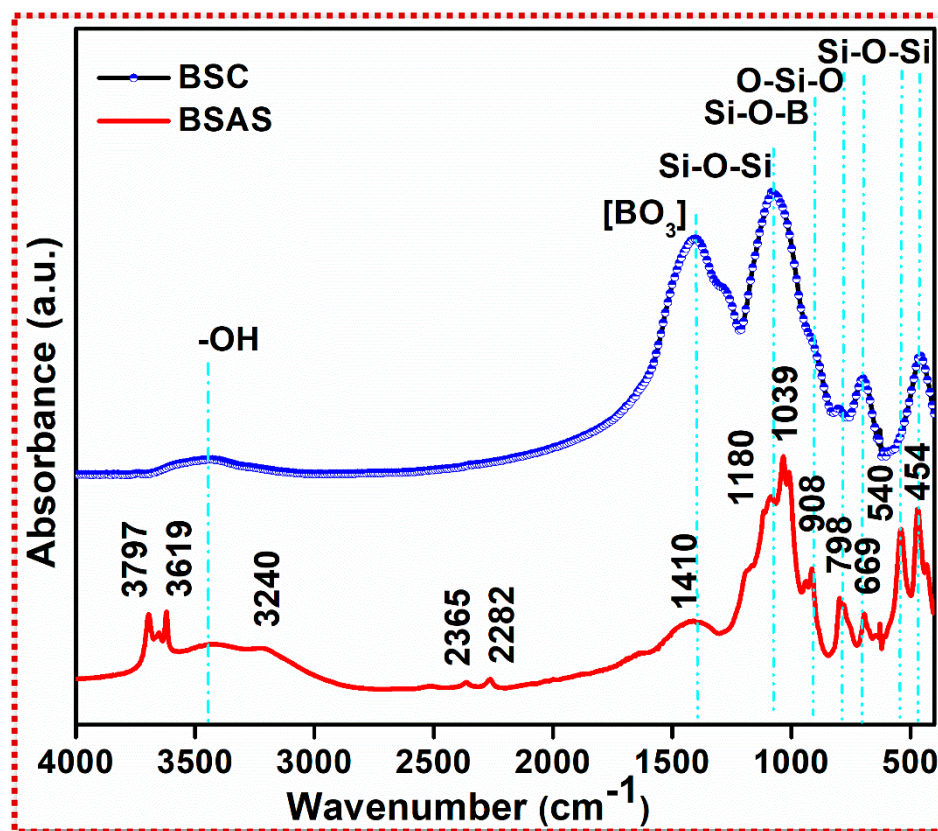


Figure 4. FTIR spectra of BSAS and BSC samples.

3.4. Morphological Analysis

The scanning electron microscopy (SEM) images obtained for the BSAS and BSC samples are displayed in Figure 5. The electron microscopy images demonstrated that, after 14 h of thermal treatment, the calcined sample (BSC) presented a smooth texture on its surface, which can be attributed to the evaporation and/or diffusion of boric acid and sodium tetraboride, which initially (Figure 5a) were presented in a powder form covering the SiO_2 particles, and after calcination, disappeared considerably (Figure 5b); these results can also be reflected with the elemental composition analysis (in weight %) and are summarized in Table 1.

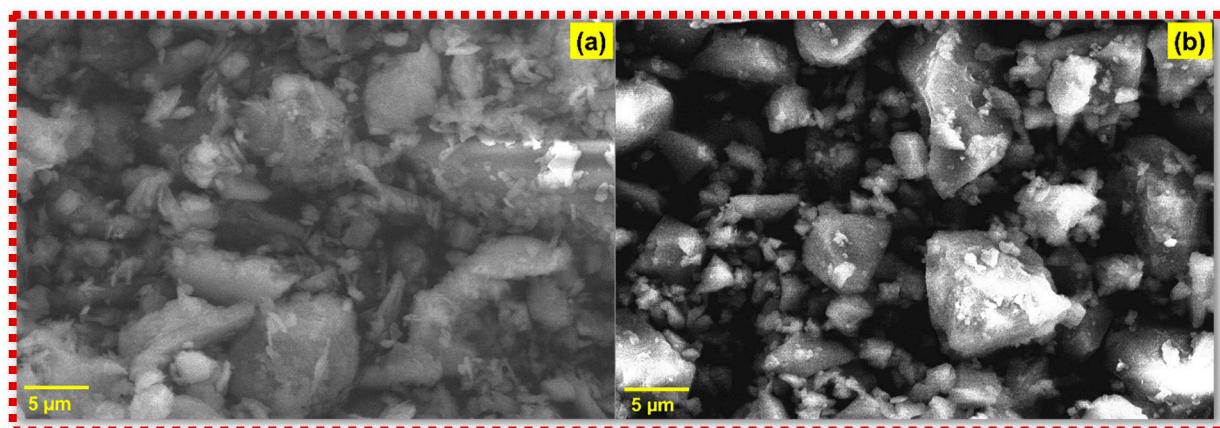


Figure 5. SEM images: (a) BSAS and (b) BSC.

Table 1. Elemental composition analysis of the samples in weight %.

Elements	Samples	
	BSAS	BSC
B	0.29	0.17
C	12.54	7.71
O	45.86	55.96
Na	0.47	0.12
Mg	0.84	0.8
Al	9.95	6.07
Si	30.05	29.17
Total	100	100

3.5. Antibacterial Activity

According to the results displayed in Table 2, after 72 h, during which time the samples were left to wait for the growth of *E. coli* bacteria, it was observed that there was growth resistance of *E. coli* bacteria to the combined action of BSC and chloramphenicol. Although it was observed in all cases that the bacteria recovered and resisted up to double on the third day, in the case of sample 7, in which only chloramphenicol was acting, it could be observed that the number of microorganisms concentrated on the third day was lower than that for all the other samples mentioned, which means that it presented certain sensitivity to bacterial attack, because, in the three repetitions, it exhibited the lowest proliferation indexes. It was also observed in both samples 1 and 7 that the proliferation was lower, which meant that chloramphenicol and the BCS acted alone, independently of each other, and were more effective against the microorganism.

Table 2. *E. coli* counts against chloramphenicol and BSC.

Independent Variable			Dependent Variable			Remarks
<i>E. coli</i> ATCC 25922 WDCM 0013	Initial Inoculum		790,000 CFU/mL			
Sample No.	BSC (µg/mL)	Chloramphenicol (µg/mL)	24 h Count (CFU/mL)	48 h Count (CFU/mL)	72 h Count (CFU/mL)	
1	0	20	8.1×10^{12}	4.6×10^{12}	5.9×10^{12}	None
2	8	20	7.2×10^{12}	4.9×10^{12}	8.3×10^{12}	None
3	12	20	8.6×10^{12}	3.6×10^{12}	6.2×10^{12}	None
4	16	20	6.8×10^{12}	5.7×10^{12}	7.4×10^{12}	None
5	20	20	3.9×10^{12}	6.3×10^{12}	7.9×10^{12}	None
6	24	20	8.4×10^{12}	5.4×10^{12}	7.1×10^{12}	None
7	20	0	5.6×10^{12}	3×10^{12}	4.5×10^{12}	None
8 (White) C/inoculum	0	0	4.7×10^{12}	6.4×10^{12}	7.8×10^{12}	Increased turbidity
Negative control s/inoculum	0	0	<1	<1	<1	None

The results of the first phase showed that only sample 7, whose concentration was 20 µg/mL, presented a positive bacteriostatic or inhibitory reaction of the substance of the compound towards the strain. To study the effect of the BSC concentration on antimicrobial activity, different concentrations of BSC were inoculated and the results are provided in Table 3; in this stage, the concentrations were between 8 and 40 µg/mL. From the analysis of the results, it could be observed that the behavior of bacterial growth was similar for the nine samples at the end of the first day (column 1). The exponential growth was defined from the day of inoculation (column 1) until the second day of incubation (column 2), corresponding to 48 h of post-inoculation. From the last time (column 3) or 72 h, an incipient stationary phase was established in samples 6 and 7, because the antimicrobial

effect was slight from the second day (after 48 h), and from the third day, it began to decrease—this can be seen with greater certainty. Increasing the concentration between 36 and 40 µg/mL practically accentuated the decrease in the bacterial population, as the antimicrobial effect commenced from the first day.

Table 3. Determination of the favorable MIC range.

Sample	Description	Dosage by Weight (µg/mL)	Column 1 First Day (CFU/mL) 24 h Count	Column 2 Second Day (CFU/mL) 48 h Count	Column 3 Third Day (CFU/mL) 72 h Count	Remarks
1	BSC	8	8.1×10^{12}	8.5×10^{12}	7.8×10^{12}	No antimicrobial effect
2		12	8.1×10^{12}	8.4×10^{12}	7.4×10^{12}	No antimicrobial effect
3		16	8.1×10^{12}	8.4×10^{12}	6.5×10^{12}	Low antimicrobial effect
4		20	7.5×10^{12}	8.3×10^{12}	5.6×10^{12}	Low antimicrobial effect
5		24	8.1×10^{12}	8.4×10^{12}	3.0×10^{12}	Moderate antimicrobial effect
6		28	8.1×10^{12}	7.5×10^{12}	2.8×10^{12}	Moderate antimicrobial effect
7		32	8.0×10^{12}	7.3×10^{12}	2.8×10^{12}	Moderate antimicrobial effect
8		36	8.1×10^{12}	7.2×10^{12}	2.5×10^{12}	High antimicrobial effect
9		40	7.2×10^{12}	7.0×10^{12}	2.5×10^{12}	High antimicrobial effect

The objective was to determine, study, and evaluate the microbiological parameter of MIC applied to BSC against *E. coli* in order to identify the range of concentrations, in µg/mL, that minimally comply with the property of inhibition of its growth and proliferation; thus, other tasks had to be previously fulfilled. First, after the use of different concentrations in 10 mL of culture medium after 72 h of incubation at 37 °C, dilution in tubes, incubation in the tubes, subsequent seeding in Petri dishes, and final count were required both in the first and second stage (Figure 1); second, the quantity of *E. coli* in CFU/mL identified and accumulated in the BSC after performing the study of both stages was determined. Finally, in the third stage, a comparison was made with another antibiotic substance to determine the antibacterial activities of the samples against *E. coli* compared with chloramphenicol and a statistical analysis was performed.

3.6. Statistical Analysis

The simple ANOVA statistical method was used to perform the statistical analysis of the synthesized samples. The average or means for three repetitions of each concentration were calculated for every 24 h, and with these data, the quantitative data of bacterial growth were estimated; this was performed in both the cases of the first and the second stages of the samples. The normality plot for the interaction between borosilicate enamel powder and chloramphenicol against *E. coli* shows the growth of colonies. It was considered a “moment analysis” (Figure 6), which allowed us to express the measurement of certain bacteriostatic activity for each of the concentrations of ground borosilicate compound. The experiments were carried out with strict rigorousness, and the estimated graph allowed us to gain an understanding of the expected behavior of the effectiveness of this compound.

In the specific case of this manuscript, it was found that the borosilicate compound did not have a bactericidal effect. For that reason, the method called “the death curve or lethality” was not developed. This would be convenient for later research. It is necessary and requires more time points to know the precise time of extermination, so a period of 72 h was considered [26,27]. In this way, the kinetics of bacterial death were measured by counting the number of colonies that remained alive after exposure to the borosilicate compound in relation to the original inoculum. In the second stage, the same procedures as those carried out in the first stage were used. The “stationary” trend plot was used for the powdered borosilicate compound. The counts obtained are expressed in CFU/mL.

Following the simple ANOVA statistical methodology, the results obtained were at a significance level of $\alpha < 5\%$ to determine whether the procedure employed was correctly stated and could be used in similar studies. Thus, before performing the analysis, it was necessary to check two important assumptions (normality and the heteroscedasticity

test); therefore, hypothesis contrast was performed without any problem. The data were recorded on data record cards, which were processed and arranged in results tables. In the analysis and interpretation of the information, the evaluation of the bacteriostatic effect was performed through the statistical analysis of the data. An ANOVA analysis was performed, with a p of 0.05, to check if there was a statistical difference between the treatment groups, and Tukey's test of differentiation was used to compare the means of each treatment group.

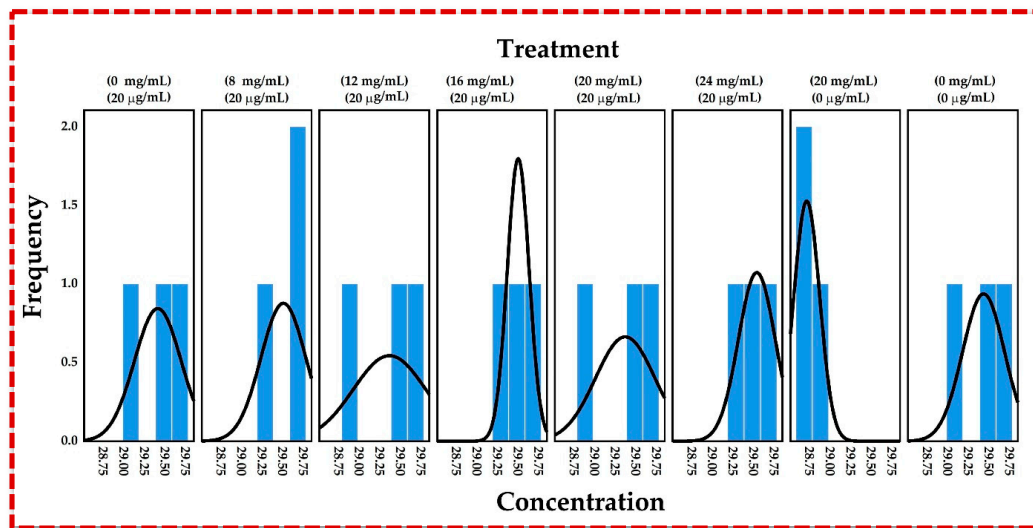


Figure 6. Normality plot for the interaction between borosilicate enamel powder and chloramphenicol.

3.6.1. Validation of the Method Determining Bacteriostatic Effect of the First Stage of Research Using Chloramphenicol and BSC at the Same Time

The result of the statistical analysis of this first stage showed that the chloramphenicol, together with the “powdered borosilicate compound (PBC)”, did not exert a synergistic action against the *E. coli* bacteria. Ultimately, it can be noticed that both composites did not have a positive effect on decreasing the microorganism population. The normality assumption for the interaction between the composites is provided in Table 4.

1. Normality assumption:

Formulation of statistical hypothesis at 5%.

Null hypothesis: The concentration of microorganisms has a normal distribution.

Alternate hypothesis: The concentrations of microorganisms do not have a normal distribution.

According to the rule for contracting the hypotheses, if the significance is greater than 5%, then the null hypothesis is not rejected and if it is less than or equal to 5%, then the null hypothesis is rejected. According to Table 4, it is observed that the significance or p -value showed results above 5% or 0.05; consequently, the null hypothesis was confirmed—the concentrations of microorganisms had a normal distribution for the interaction between borosilicate and chloramphenicol in the eight treatments. The normality test (plots) for the eight treatments is shown in Figure 6.

Table 4. Normality assumption for the interaction between borosilicate and chloramphenicol.

Treatment	Statistics	gl	Sig.
(0 mg/mL) (20 µg/mL)	0.995	3	0.868
(8 mg/mL) (20 µg/mL)	0.934	3	0.504
(12 mg/mL) (20 µg/mL)	0.980	3	0.728
(16 mg/mL) (20 µg/mL)	0.960	3	0.617
(20 mg/mL) (20 µg/mL)	0.959	3	0.610
(24 mg/mL) (20 µg/mL)	0.981	3	0.738
(20 mg/mL) (0 µg/mL)	0.843	3	0.222
(0 mg/mL) (0 µg/mL)	0.984	3	0.760

2. Heteroscedasticity assumption

This applies to the interaction between borosilicate enamel powder and chloramphenicol. Formulation of statistical hypothesis at 5%.

Null hypothesis: The concentrations of microorganisms had homoscedastic data.

Alternative hypothesis: The concentrations of microorganisms did not have heteroscedastic data.

According to Table 5, it was observed that the significance or p -value showed data above 5% or 0.05, (0.553, 0.883, 0.879, and 0.577); consequently, the null hypothesis was confirmed, i.e., the concentrations of microorganisms had homoscedastic data. In effect, after demonstrating the two assumptions of normality and homoscedasticity, and consequently, after fulfilling the assumptions, it was necessary to perform the analysis of variance.

Table 5. Test for homogeneity of variances.

	Levene's Statistic	gl1	gl2	Sig.
Based on the mean	0.866	7	16	0.553
Based on the median	0.408	7	16	0.883
Based on the median and with adjusted Gl	0.408	7	11.490	0.879
Based on the trimmed mean	0.831	7	16	0.577

3. Analysis of variance

Formulation of statistical hypothesis at 5%.

Null hypothesis: The concentration of microorganisms had a normal distribution.

Alternate hypothesis: The concentrations of microorganisms did not have a normal distribution.

According to Table 6, it was observed that the significance or p -value showed data above 5% or 0.05, which meant that $0.048 < 0.05$; consequently, the alternative hypothesis was confirmed, i.e., there was a difference in the microorganism's concentrations.

Table 6. Analysis of variance for microorganism concentrations.

	Sum of Squares	gl	Root Mean Square (RMS)	F	Sig.
Between groups	1.491	7	0.213	2.682	0.048
Within groups	1.271	16	0.079		
Total	2.762	23			

Table 7 shows the differences between the eight treatments, and it was observed that the interactions of the powdered borosilicate compound (PBC) and chloramphenicol (20 and 0 $\mu\text{g/mL}$) showed a higher average for the rest of the treatments, confirming the proposed hypothesis. Further, the hypothesis confirmed that the resistance activity of the synthesized PBC functioned efficiently against *E. coli* attack and was interpreted through the quantities of microorganism concentrations that were confirmed when inoculated into the compound (Figure 7).

Table 7. Duncan's test for the difference between the interactions of the concentrations of microorganisms.

Treatment	N	Subset for Alpha = 0.05	
		1	2
(20 mg/mL) (0 $\mu\text{g/mL}$)	3	28.7323	
(12 mg/mL) (20 $\mu\text{g/mL}$)	3		29.3835
(20 mg/mL) (20 $\mu\text{g/mL}$)	3		29.3872
(0 mg/mL) (20 $\mu\text{g/mL}$)	3		29.4287
(0 mg/mL) (0 $\mu\text{g/mL}$)	3		29.4503
(16 mg/mL) (20 $\mu\text{g/mL}$)	3		29.5173
(8 mg/mL) (20 $\mu\text{g/mL}$)	3		29.5242
(24 mg/mL) (20 $\mu\text{g/mL}$)	3		29.5559
Sig.		1.000	0.513

It could also be observed that the joint action of the concentration of 20 µg/mL of powdered borosilicate compound and 8 µg/mL of chloramphenicol against *E. coli* presented a slight tendency to increase the proliferation of the *E. coli* strain (Figure 7). The obtained value was 29.52 and it belonged to sample 7. Figure 7 is a graphic representation of Table 7, where the growth stages of the *E. coli* bacteria in the respective Petri dishes from left to right can be visualized through the images of the average of the three days of growth of each of the groupings. Therefore, there was no synergy between chloramphenicol and BSC.

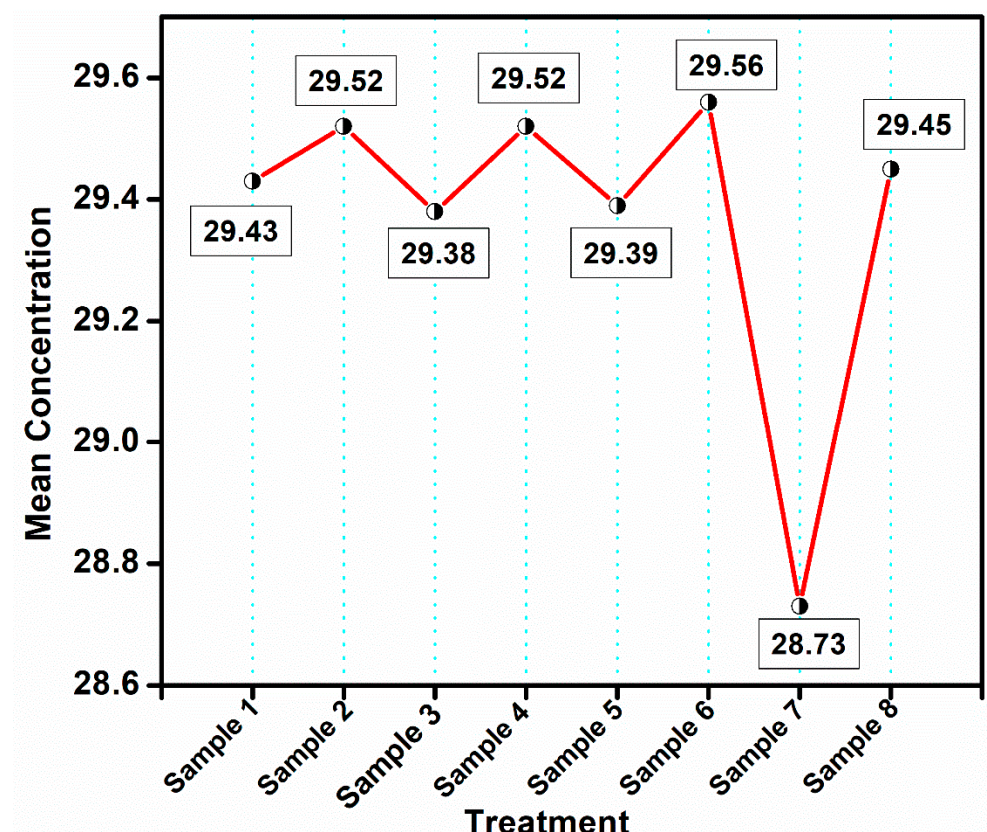


Figure 7. Graph presenting the values obtained from Table 7.

3.6.2. Validation of the Statistical Method That Determined the Bacteriostatic Effect of BSC with Concentrations of 28–40 mg/mL

1. Normality assumption

Formulation of statistical hypothesis at 5%.

According to Table 8, it was observed that the significance or *p*-value showed data above 5% or 0.05; consequently, the null hypothesis was confirmed—the concentrations of microorganisms had a normal distribution for the borosilicate compound.

Table 8. Normality assumption for the three days on initial inoculum growth.

Day	Kolmogorov–Smirnov			Shapiro–Wilk		
	Statistics	gl	Sig.	Statistics	gl	Sig.
First day	0.370	9	0.001	0.618	9	0.060
Second day	0.301	9	0.018	0.804	9	0.053
Third day	0.309	9	0.013	0.804	9	0.073

2. Heteroscedasticity assumption

Formulation of statistical hypotheses at 5%.

According to Table 9, it was observed that the significance or *p*-value showed data above 5% or 0.05; consequently, the null hypothesis was confirmed, i.e., the growth of the initial inoculum of microorganisms had homoscedastic data. In effect, after demonstrating the two assumptions of normality and homoscedasticity, after fulfilling the assumptions, it was necessary to perform the analysis of variance.

Table 9. Homoscedasticity assumption for the interaction between borosilicate and chloramphenicol.

	Levene's Statistic	gl1	gl2	Sig.
Based on the mean	47.887	2	24	0.073
Based on the median	4.981	2	24	0.066
Based on the median and with adjusted Gl	4.981	2	9.598	0.053
Based on the trimmed mean	43.632	2	24	0.045

3. Analysis of variance

Formulation of statistical hypothesis at 5%.

Null hypothesis: There was no difference in the three days of initial inoculum growth.

Alternative hypothesis: There was a difference in the three days of initial inoculum growth.

According to Table 10, it was observed that the significance or *p*-value showed data below 5% or 0.05, i.e., $0.000 < 0.05$; consequently, the alternative hypothesis was confirmed—there was a difference in the three days on initial inoculum growth.

Table 10. Analysis of variance for the three days on initial inoculum growth.

Source of Variation	Sum of the Squares	gl	Root Mean Square	F	Sig.
Between groups	6778.741	2	3389.370	18.277	0.000
Within groups	4450.667	24	185.444		
Total	11,229.407	26			

Table 11 shows the differences between the three days on initial inoculum growth; it was observed that there was a difference for the third day with respect to the first and second days. For instance, the first day showed an average growth of 79.22, while for the second day, it showed an average of 78.89, which was similar to the growth of the first day; meanwhile, for the third day, it showed a growth below the first and second day, with an average growth of 45.44, thus confirming the results obtained in the ANOVA table, which shows that there was a significant difference for the three days of initial inoculum growth.

Table 11. Duncan's test for the difference between the three days of initial inoculum growth.

Day	N	Subset for Alpha = 0.05	
		1	2
Third day	9	45.4444	
Second day	9		78.8889
First day	9		79.2222
Sig.		1.000	0.959

Figure 8 confirms the results obtained in Tables 10 and 11, in which there is a significant difference in the three days (Figure 8a), as well as the difference in the third day with respect to the first and second days. Figure 8b shows the trend toward a “steady state” for the concentration of the proposed borosilicate enamel powder, which showed a decreasing trend on average as the borosilicate increased from 8.00 mg/mL, with 81 of initial inoculum growth, until reaching 40.00 mg/mL, showing an average value of 26 initial inoculum growth, thus showing a decrease. In conclusion, the obtained results were significant, with

the optimized concentration range of 28 to 32 mg/mL, which was determined to be the MIC for the synthesized borosilicate compound and was also considered to be valid.

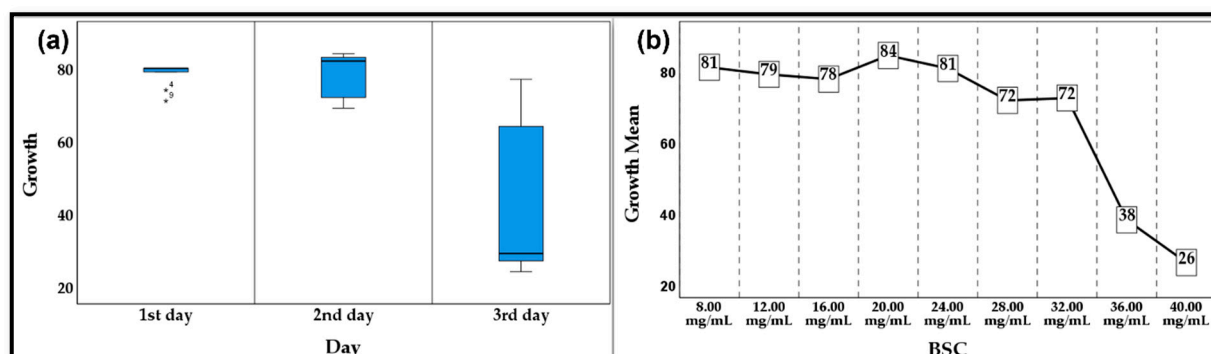


Figure 8. (a) Box plot for three-day behavior on initial inoculum growth and (b) Stationary trend plot for the powdered borosilicate compound. The *⁴ and *⁹ represent the scientific error values.

4. Discussion

This section is a discussion related to the research conducted by comparing it with the existing literature on borate compounds and chloramphenicol, the MIC procedure and inoculum size, microstructural characterization, and, finally, the validation of the results.

There are precedents on substances that have synergistic action against bacteria when applied simultaneously, for example, the context for this work was based on the successful combination of borosilicate with another antibiotic against Gram-negative bacteria by Rodriguez et al. [28]. The efficacy increased with increasing temperature. With this background, as can be seen, an antibiotic plus a borate compound was used to combat *E. coli*, producing positive results, with a minimum concentration of 8 mg/mL to act on inhibiting the bacteria. However, to comply with the sanitary regulations, a concentration of 16 mg/mL was used. An antibiotic that maintains synergy with other compounds against bacteria is chloramphenicol, which is mainly used to combat the bacteria that cause typhoid fever, brucellosis, and bronchopulmonary infections; it is also not used to combat candidiasis, which is the urinary tract infection corresponding to the diseases caused by *E. coli* [29]. There are also studies in which synergy is achieved against Gram-negative bacteria, based on colistin and working together [18].

Based on the consideration of the previous results closer to the present study [8,16,17], in which the interaction between borate compounds and chloramphenicol was mentioned, interesting methodologies were developed to treat bacteria, such as *E. coli*, by means of using chloramphenicol through the performance of a series of tests to characterize the stereoselective metabolism of chloramphenicol by bacterial strains isolated from influent wastewater containing the chloramphenicol acetyltransferase gene in order to purify polluted river water and neutralize all types of contaminants, whether chemical or biological, and obtain water suitable for the human consumption. The content of the inoculum was obtained from a powdered mixture containing the borosilicate compound (BSC) with a smaller portion of the drug “chloramphenicol” to reinforce the inhibitory action (Table 2); in this work, an inoculum volume of 1 mL was used, as established by standards [30], which was an initial amount of 790,000 active microorganisms. The experimentation results were proposed as the use of a biocidal compound allied to the borosilicate compound, such as chloramphenicol (Figure 1), and therein lies the novelty of the experimentation process of this work, since, by using the two substances with a broad biocidal spectrum, it was expected to have a positive result in the extermination of a greater number of *E. coli*. However, during the experimentation, an analysis specimen containing only the amorphous powdered compound diluted in peptone was also considered, facing only *E. coli*. Regarding the volume of the inoculum of this strain to start the experimentation, the established standards were taken into account, which specified that the size of the inoculum volume for

chloramphenicol should not exceed 1 to 2 μL and that the concentration of microorganisms should not exceed 10^4 CFU to work within the range of MIC in compounds that are similar to that of chloramphenicol. Thus, they also experimented with inoculum that had a volume of 20 μL of chloramphenicol to deal with *E. coli*, obtaining good results [31–33]. Similar designs to their volumes and concentrations of the inoculum, without restrictions of any norm, established the size of the inoculum to be 5.5×10^5 cells per mL (Table 2).

In the first part of the methodology, it was tested that the powdered borosilicate compound (BSC) combined with chloramphenicol could inhibit or exterminate these bacteria. However, after the experimental processes and the respective analysis in a certified laboratory, it was found that, from a series of 8 samples, including blanks, etc., the borosilicate compound combined with its ally “chloramphenicol” did not effectively reduce the concentration of microorganisms. It was also interesting to note that sample 1, which only contained chloramphenicol acting alone against the strain, did not control the growth, including the proliferation, of *E. coli*; it was more abundant than what was produced in the borosilicate compound when it acted alone against *E. coli*. It is interpreted from the results that neither chloramphenicol nor borosilicate acting alone were able to stop the microorganism proliferation. This was possible because the pre-established concentration of chloramphenicol was very low, despite the fact that the standards already studied [34,35] established not to go out of the range of 2 to 8 $\mu\text{g/L}$ or use ranges lower than 20 $\mu\text{g/L}$. Additionally, the exact initial quantity of active microorganisms that should be used to start the analysis has not been established as a norm and the quantity of the borosilicate compound was very low for this concentration of active microorganisms. In the final stage (Table 3) of the experimentation, with the use of various concentrations of powdered amorphous borosilicate compound between 8 and 40 $\mu\text{g/mL}$, it was finally possible to determine the range that allowed finding the signs of a sustained reduction in the proliferation of *E. coli*, which was between 28 and 32 $\mu\text{g/mL}$, the one that evidenced such behavior. The process went through 3 phases. In the first one, the extermination effect just began as it was in metabolic competition. Then, it passed to the state of an increasing inhibitory effect, and finally, in the concentration of 40 $\mu\text{g/mL}$, the result was more evident regarding the inhibitory effect as it began from the first day, which allowed us to conclude that this value would be the most beneficial to be used as an antibiotic as it was the most effective in the phase of exponential growth of *E. coli*. (Table 11 and Figure 8).

In this research work, a procedure was developed that could determine the antibacterial properties and the MIC using the BSC against *E. coli*. With respect to the procedure developed, the methodology paves an avenue for designing new drugs inspired by other substances, such as BSC. Following the technique of using inoculum in dilution in 10 mL tubes, using the substance of BSC in this study, ground and diluted in peptone at various concentrations between 28 and 40 $\mu\text{g/mL}$ [36], it was also concluded from the results obtained and compared with the other procedures presented above that it was capable of resisting *E. coli* and maintaining this MIC against the microorganism. The results of this study demonstrated that the BSC had a positive prognostic bacteriostatic effect against the bacterium *E. coli*, but only when it acted “alone” against the strain and at higher concentrations between 28 and 40 $\mu\text{g/mL}$. As a final caution, BSC exerts its antibiotic action effectively from the SiO_2 in the cristobalite phase to inhibit biological contaminants, such as *E. coli*, in the antibacterial application according to the results of the microstructure characterization analysis, the sensitivity tests, and having contrasted our results with other antecedents found in the current state of the art.

However, neither the use of drugs obtained from polymorphs and amorphous solids for the specific treatment of *E. coli* bacteria, nor the applications of borate substances combined with amorphous solids to form antibiotics, have been reported in pharmacology. In this study, the calcined borosilicate compound (BSC) was subjected to XRD analysis to determine the presence of crystalline solids, and it was found that 62.1% of the material was quartz, 6.6% was cristobalite, and 31% was an amorphous phase that could be primarily attributed to SiB_6 by FTIR spectroscopy. Further, the obtained results lead us to investigate

within the state of the art that other silicate-derived compounds have pharmacological action against *E. coli*, since immunosensors [37], based on a quartz crystal microbalance (QCM), have been developed for the detection of *Vibrio harveyi* (*V. harveyi*), a pathogenic bacterium that causes morbidity and even a high level of mortality in commercial shrimp cultures, including *Penaeus monodon*; this was achieved through the immobilization of a monoclonal antibody (MAb) against *V. harveyi*. This result, unlike that developed in the current work, uses grinding with granulometry at the level of nanoparticles.

5. Conclusions

A borosilicate compound (BSC) was synthesized using natural and recycled materials with incipient antibacterial efficacy. The X-ray diffraction results and the Rietveld refinement method showed that the synthesized BSC material was composed of 62.10% quartz, 6.6% cristobalite, and 31.1% amorphous phase. Further, the obtained FTIR results complemented the XRD results, indicating that the amorphous phase corresponded mainly to SiB_6 . The antimicrobial activity studies showed that the chloramphenicol and BSC performed better individually than together, managing to inhibit bacterial growth from 7.8×10^{12} CFU/mL in the blank to 5.9×10^{12} CFU/mL and 4.5×10^{12} CFU/mL, respectively. It was the combined antimicrobial activity of the BSC components (quartz, cristobalite, and silicon hexaboride) that contributed to the greater inhibition of *E. coli*. The MIC of the BSC that presented greater antimicrobial inhibition against *E. coli* and was found to be 36 $\mu\text{g/mL}$, where, after 72 h, the colony-forming units were reduced to 2.5×10^{12} (CFU/mL) according to the trend presented in the evaluation days, and it was observed that, with a longer evaluation time, the inhibition would increase or even eliminate *E. coli* altogether. The most suitable MIC concentration for an efficient “antibacterial material against *E. coli*” was in the range of 28 to 40 $\mu\text{g/mL}$. Also, the ANOVA analysis confirmed that the results were reliable because there was a significant difference in the period of initial inoculum growth; the accurate MIC values were between 28 and 32 $\mu\text{g/mL}$.

6. Patent

This article has a patent as a request for processing in INDECOPI Peru with Number 000438-2022/DIN-Peru.

Author Contributions: Conceptualization and original idea, B.S.V.B.; experimentation, B.S.V.B. and I.d.C.E.R.; methodology, B.S.V.B. and T.C.d.T.; software, L.A.L.A.; validation, B.S.V.B., F.d.C.D. and J.A.A.M.; Analytical analysis of the samples, E.J.S.S.; review and editing, R.V.M. and A.A.; formal analysis, B.S.V.B.; investigation, B.S.V.B. and I.d.C.E.R.; resources, B.S.V.B.; data curation, F.d.C.D.; writing—original draft preparation, T.C.d.T., R.V.M. and A.A.; writing—review and editing, B.S.V.B., A.A. and R.V.M.; visualization, J.A.A.M.; supervision, J.A.A.M. All authors have read and agreed to the published version of the manuscript.

Funding: This research was funded by the Universidad Nacional de Moquegua through “Fondos del Canon y Sobrecanon, Regalías, Renta de Aduanas”, and approved with resolution of the organizing commission N° 352-2022-UNAM, with the project “caracterización micro-estructural de un antibiótico boratado, obtenido de boro residual, y su aplicación en el diseño de recubrimientos fotocatalíticos urbanos antibacterianos”.

Data Availability Statement: Data available on request due to restrictions.

Conflicts of Interest: Author I.d.C.E.R. was employed by the company ONG Waykay. The remaining authors declare that the research was conducted in the absence of any commercial or financial relationships that could be construed as a potential conflict of interest.

References

1. Younsi, A.; Mahi, M.A.; Hamami, A.E.A.; Belarbi, R.; Bastidas-Arteaga, E. High-Volume Recycled Waste Glass Powder Cement-Based Materials: Role of Glass Powder Granularity. *Buildings* **2023**, *13*, 1783. [\[CrossRef\]](#)
2. Larionau, P.; Hujova, M.; Michalková, M.; Mahmoud, M.; Švančárková, A.; Galusková, D.; Parchoviansky, M.; Bernardo, E.; Galusek, D.; Kraxner, J. Low-alkali borosilicate glass micro-spheres from waste cullet prepared by flame synthesis. *Int. J. Appl. Glas. Sci.* **2021**, *12*, 562–569. [\[CrossRef\]](#)
3. Ramteke, D.D.; Hujova, M.; Kraxner, J.; Galusek, D.; Romero, A.R.; Falcone, R.; Bernardo, E. Up-cycling of ‘unrecyclable’ glasses in glass-based foams by weak alkali-activation, gel casting and low-temperature sintering. *J. Clean. Prod.* **2021**, *278*, 123985. [\[CrossRef\]](#)
4. Gin, S.; Guo, X.; Delaye, J.-M.; Angeli, F.; Damodaran, K.; Testud, V.; Du, J.; Kerisit, S.; Kim, S.H. Insights into the mechanisms controlling the residual corrosion rate of borosilicate glasses. *Npj Mater. Degrad.* **2020**, *4*, 41. [\[CrossRef\]](#)
5. Lonergan, J.M.; Lonergan, C.; Silverstein, J.; Cholsaipant, P.; McCloy, J. Thermal properties of sodium borosilicate glasses as a function of sulfur content. *J. Am. Ceram. Soc.* **2020**, *103*, 3610–3619. [\[CrossRef\]](#)
6. Luo, Y.; Bao, S.; Zhang, Y. Recycling of granite powder and waste marble produced from stone processing for the preparation of architectural glass–ceramic. *Constr. Build. Mater.* **2022**, *346*, 128408. [\[CrossRef\]](#)
7. Fabert, M.; Ojha, N.; Erasmus, E.; Hannula, M.; Hokka, M.; Hyttinen, J.; Rocherullé, J.; Sigalascd, I.; Massera, J. Crystallization and sintering of borosilicate bioactive glasses for application in tissue engineering. *J. Mater. Chem. B* **2017**, *5*, 4514–4525. [\[CrossRef\]](#) [\[PubMed\]](#)
8. Fink, K.; Uchman, M. Boron cluster compounds as new chemical leads for antimicrobial therapy. *Co-Ord. Chem. Rev.* **2021**, *431*, 213684. [\[CrossRef\]](#)
9. Thorley, N.; Ross, J. Intravaginal boric acid: Is it an alternative therapeutic option for vaginal trichomoniasis? *Sex Transm. Infect.* **2018**, *94*, 574–577. [\[CrossRef\]](#)
10. García-García, J.A.; Azofeifa-Bolaños, J.B. Efecto del ácido bórico y la luz en el número y biomasa de microtubérculos de papa cv. “Floresta”. *Uniciencia* **2017**, *31*, 121. [\[CrossRef\]](#)
11. Kumar, A.; Mittal, A.; Das, A.; Sen, D.; Mariappan, C.R. Mesoporous electroactive silver doped calcium borosilicates: Structural, anti-bacterial and myogenic potential relationship of improved bio-ceramics. *Ceram. Int.* **2021**, *47*, 3586–3596. [\[CrossRef\]](#)
12. Balestriere, M.; Schuhladden, K.; Seitz, K.H.; Boccaccini, A.; Cere, S.; Ballarre, J. Sol-gel coatings incorporating borosilicate bioactive glass enhance anti corrosive and surface performance of stainless steel implants. *J. Electroanal. Chem.* **2020**, *876*, 114735. [\[CrossRef\]](#)
13. Kumar, A.; Mariappan, C. A new biocompatible phosphate free mesoporous calcium borosilicate glass-ceramics for medical application. *Mater. Lett.* **2021**, *305*, 130752. [\[CrossRef\]](#)
14. Kayani, Z.N.; Bashir, Z.; Mohsin, M.; Riaz, S.; Naseem, S. Sol-Gel Synthesized Boron nitride (BN) Thin Films for Antibacterial and Magnetic Applications. *Optik* **2021**, *243*, 167502. [\[CrossRef\]](#)
15. Arciénaga, I.M.; Moraga, N.B.; Rajal, V.B.; Romano Armada, N. Influencia del ácido bórico sobre propiedades promotoras de creci-miento vegetal de *Pseudomonas putida* KT2440. *Agrotecnia* **2017**, *25*, 41. [\[CrossRef\]](#)
16. Drago, L. Chloramphenicol Resurrected: A Journey from Antibiotic Resistance in Eye Infections to Biofilm and Ocular Micro-biota. *Microorganisms* **2019**, *7*, 278.
17. Tevyashova, A.N. Recent Trends in Synthesis of Chloramphenicol New Derivatives. *Antibiotics* **2021**, *10*, 370. [\[CrossRef\]](#) [\[PubMed\]](#)
18. Wei, W.-J.; Yang, H.-F. Synergy against extensively drug-resistant *Acinetobacter baumannii* in vitro by two old antibiotics: Colistin and chloramphenicol. *Int. J. Antimicrob. Agents* **2017**, *49*, 321–326. [\[CrossRef\]](#)
19. Altaf, M.; Ijaz, M.; Ghaffar, A.; Rehman, A.; Avais, M. Antibiotic susceptibility profile and synergistic effect of non-steroidal anti-inflammatory drugs on antibacterial activity of resistant antibiotics (Oxytetracycline and Gentamicin) against methicillin resistant *Staphylococcus aureus* (MRSA). *Microb. Pathog.* **2019**, *137*, 103755. [\[CrossRef\]](#)
20. Sevim, F.; Demir, F.; Bilen, M.; Okur, H. Kinetic analysis of thermal decomposition of boric acid from thermogravimetric data. *Korean J. Chem. Eng.* **2006**, *23*, 736–740. [\[CrossRef\]](#)
21. Pignatelli, G.; Queirolo, G. Further insight on boron diffusion in silicon obtained with Auger electron spectroscopy. *Thin Solid Film.* **1980**, *67*, 233–238. [\[CrossRef\]](#)
22. Xie, F.; Juan, I.G.; Arango-Ospina, M.; Riedel, R.; Boccaccini, A.R.; Ionescu, E. Apatite Forming Ability and Dissolution Behavior of Boron- and Calcium-Modified Silicon Oxycarbides in Comparison to Silicate Bioactive Glass. *ACS Biomater. Sci. Eng.* **2019**, *5*, 5337–5347. [\[CrossRef\]](#)
23. Degen, T.; Sadki, M.; Bron, E.; König, U.; Nénert, G. The HighScore suite. *Powder Diff.* **2014**, *29*, S13–S18. [\[CrossRef\]](#)
24. D’Souza, M.J.; Koyoshi, F. Extracting Relevant Information from FDA Drug Files to Create a Structurally Diverse Drug Database Using KnowItAll®. *Pharm. Rev.* **2009**, *7*, 1–15.
25. Munno, K.; De Frond, H.; O’donnell, B.; Rochman, C.M. Increasing the Accessibility for Characterizing Microplastics: Introducing New Application-Based and Spectral Libraries of Plastic Particles (SLoPP and SLoPP-E). *Anal. Chem.* **2020**, *92*, 2443–2451. [\[CrossRef\]](#) [\[PubMed\]](#)
26. Messori, A. Survival curve fitting using the Gompertz function: A methodology for conducting cost-effectiveness analyses on mortality data. *Comput. Methods Programs Biomed.* **1997**, *52*, 157–164. [\[CrossRef\]](#)
27. Yu, H.; Wehrhahn, M. Implementation of EUCAST short incubation break points directly from blood culture bottles in a private microbiology laboratory. *Pathology* **2020**, *52*, S128. [\[CrossRef\]](#)

28. Rodriguez, O.; Stone, W.; Schemitsch, E.H.; Zalzal, P.; Waldman, S.; Papini, M.; Towler, M.R. Titanium addition influences antibacterial activity of bioactive glass coatings on metallic implants. *Heliyon* **2017**, *3*, e00420. [[CrossRef](#)]
29. Ochoa Sangrador, C.; Brezmes Raposo, M. Tratamiento antibiótico recomendado en episodios de infección urinaria. *Pediatría* **2007**, *67*, 485–497. [[CrossRef](#)] [[PubMed](#)]
30. Buffet-Bataillon, S.; Branger, B.; Cormier, M.; Bonnaure-Mallet, M.; Jolivet-Gougeon, A. Effect of higher minimum inhibitory concentrations of quaternary ammonium compounds in clinical *E. coli* isolates on antibiotic susceptibilities and clinical outcomes. *J. Hosp. Infect.* **2011**, *79*, 141–146. [[CrossRef](#)]
31. Demirel, B.; Taygun, M.E. Antibacterial Borosilicate Glass and Glass Ceramic Materials Doped with ZnO for Usage in the Pharmaceutical Industry. *ACS Omega* **2023**, *8*, 18735–18742. [[CrossRef](#)]
32. Canovas, J.; Petitjean, G.; Chau, F.; Le Monnier, A.; Fantin, B.; Lefort, A. Expression of CTX-M-15 limits the efficacy of ceftolozane/tazobactam against *Escherichia coli* in a high-inoculum murine peritonitis model. *Clin. Microbiol. Infect.* **2020**, *26*, 1416.e5–1416.e9. [[CrossRef](#)] [[PubMed](#)]
33. Imane, N.I.; Fouzia, H.; Azzahra, L.F.; Ahmed, E.; Ismail, G.; Idrissa, D.; Mohamed, K.-H.; Sirine, F.; L'Houcine, O.; Noureddine, B. Chemical composition, antibacterial and antioxidant activities of some essential oils against multidrug resistant bacteria. *Eur. J. Integr. Med.* **2020**, *35*, 101074. [[CrossRef](#)]
34. Witt, L.S.; Spicer, J.O.; Burd, E.; Kraft, C.S.; Babiker, A. Evaluation of clinicians' knowledge and use of minimum inhibitory concentration values. *Braz. J. Infect. Dis.* **2021**, *25*, 101656. [[CrossRef](#)] [[PubMed](#)]
35. Mouton, J.W.; Muller, A.E.; Canton, R.; Giske, C.G.; Kahlmeter, G.; Turnidge, J. MIC-based dose adjustment: Facts and fables. *J. Antimicrob. Chemother.* **2018**, *73*, 564–568. [[CrossRef](#)]
36. Kowalska-Krochmal, B.; Dudek-Wicher, R. The Minimum Inhibitory Concentration of Antibiotics: Methods, Interpretation, Clinical Relevance. *Pathogens* **2021**, *10*, 165. [[CrossRef](#)]
37. Bidlas, E.; Du, T.; Lambert, R.J. An explanation for the effect of inoculum size on MIC and the growth/no growth interface. *Int. J. Food Microbiol.* **2008**, *126*, 140–152. [[CrossRef](#)] [[PubMed](#)]

Disclaimer/Publisher's Note: The statements, opinions and data contained in all publications are solely those of the individual author(s) and contributor(s) and not of MDPI and/or the editor(s). MDPI and/or the editor(s) disclaim responsibility for any injury to people or property resulting from any ideas, methods, instructions or products referred to in the content.